

Poisson-bracket formulation of the dynamics of fluids of deformable particlesArthur Hernandez¹ and M. Cristina Marchetti*Department of Physics, University of California Santa Barbara, Santa Barbara, California 93106, USA*

(Received 23 November 2020; accepted 25 February 2021; published 31 March 2021)

Using the Poisson-bracket method, we derive continuum equations for a fluid of deformable particles in two dimensions. Particle shape is quantified in terms of two continuum fields: an anisotropy density field that captures the deformations of individual particles from regular shapes and a shape tensor density field that quantifies both particle elongation and nematic alignment of elongated shapes. We explicitly consider the example of a dense biological tissue as described by the Vertex model energy, where cell shape has been proposed as a structural order parameter for a liquid-solid transition. The hydrodynamic model of biological tissue proposed here captures the coupling of cell shape to flow and provides a starting point for modeling the rheology of dense tissue.

DOI: [10.1103/PhysRevE.103.032612](https://doi.org/10.1103/PhysRevE.103.032612)**I. INTRODUCTION**

Many extended systems, such as biological tissue [1], foams [2,3], emulsions [4,5], and colloidal suspensions [4], can be described as collections of deformable particles. A variety of mesoscopic models have been developed to examine the role of particle shape on the structure and rheology of these soft materials.

Cellular Potts models [6,7] and Vertex and Voronoi models [8–10] have been successfully used to describe dry foams and confluent layers of biological tissue, where cells completely cover the plane with no gaps, with extensions to three dimensions [11,12]. These models describe cells in confluent tissues as tightly packed irregular polygons covering the plane and predict a jamming-unjamming transition tuned by a target cell shape that captures the interplay of cortex contractility and cell-cell adhesion, with the mean cell shape serving as a metric for tissue fluidity [13–15]. Vertex and Voronoi models do not, however, have a natural extension to situations where the cell packing fraction is below one, although gaps between cells have been incorporated in recent work [16,17]. In contrast, both particle deformability and density variations can be incorporated in multiphase field models and in models of deformable particles [18], which have been used to examine solid-liquid transitions as a function of both particle shape and density.

Less well developed are continuum descriptions of the rheology of materials where the constituents can change their shape. An important example is the classic work by Doi and Ohta that describes the dynamics of the interface between two immiscible fluids under shear, incorporating formation, rupture and deformation of droplets [19]. Continuum mechanics of confluent tissue have been constructed phenomenologically and employed to connect structure and mechanics in *Drosophila* development [20,21]. Ishihara and

collaborators formulated a continuum model that couples cell shape to mechanical deformations at the tissue scale [22]. Their work, however, captures only *simultaneous* cell anisotropy and alignment of elongated cell shapes, without distinguishing between a tissue where cell shapes are on average isotropic and one where cells are on average anisotropic, but not aligned, as observed in simulations of Vertex and Voronoi models [15,23]. It is in fact the single-cell anisotropy that provides an order parameter for cell jamming in Vertex and Voronoi models [13–15], where fluid states of elongated cells are obtained without nematic order of elongated cells. The importance of this distinction in a continuum theory of tissue mechanics was highlighted recently in work by one of us and collaborators [24].

In this paper we adopt the Poisson-bracket (PB) formulation [25] to obtain continuum equations for a fluid of deformable particles in two dimensions. This method has the advantage of providing a systematic derivation of the reversible part of the hydrodynamic equations once the continuum fields have been identified. Our approach is inspired by work by Stark and Lubensky [26,27] who used the PB approach to derive the hydrodynamics of a nematic liquid crystal. As in liquid crystals, we identify both a continuum scalar field that quantifies fluctuations of individual cell shape and a cell shape tensor field that captures both cell elongation and alignment. An important difference is that, while in passive liquid crystals molecular shape fluctuations decay on fast (nonhydrodynamic) timescales, numerical studies of both Vertex and Voronoi models of 2D confluent epithelial tissues [13–15] have shown that mean cell shape, as measured by the cell perimeter normalized by cell area, provides an order parameter for a transition between solid and liquid states. In the solid state cells are isotropic and encounter finite energy barriers for neighbor exchange. These barriers vanish in the liquid state, where cells acquire anisotropic shapes with large perimeters. The role of mean cell shape as a direct metric for tissue fluidity has been confirmed by experiments in various cell types [28,29]. Thus shape-anisotropy fluctuations

*Corresponding author: arthurhernandez@umail.ucsb.edu

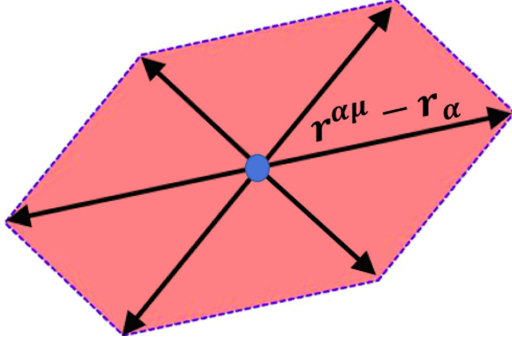


FIG. 1. A deformable particle (referred to as a “cell”) is described as an n -sided irregular polygon defined by the positions $\mathbf{r}^{\alpha\mu}$ of its vertices, for $\mu = 1, \dots, n$, relative to the location of the centroid \mathbf{r}_α of the polygon.

are long-lived near the transition, justifying the inclusion of this field in a hydrodynamic model. The equations derived here provide a continuum model for collections of interacting deformable “particles” and can be adapted to describe both confluent and nonconfluent systems.

The paper is organized as follows. In Sec. II we provide the microscopic definition of the continuum fields used in the hydrodynamic model. In Sec. III we briefly summarize the PB method and the calculation of the various PBs (with details given in Appendix C), and discuss the reactive and dissipative contributions to the coarse-grained dynamics. The final continuum equations are displayed in Sec. IV. In Sec. V we discuss the form of the continuum equations for the specific case of a cellular tissue, and conclude with a brief discussion in Sec. VI. Details of the derivation of the PBs and of the mean-field free energy of the Vertex model are given in Appendixes.

II. CONTINUUM FIELDS

We consider a fluid whose constituents are N extended particles of arbitrary shape. The contour of each particle, referred to below as a “cell,” is described by a polygonal shape joining n vertices located at \mathbf{r}^μ , where $\mu = 1, 2, \dots, n$ labels the vertices and $\alpha = 1, 2, \dots, N$ labels the cells, as shown in Fig. 1. Each cell has a total mass m_c , which we assume equally distributed among the n vertices. Note that (hence mass) proteins can often be anisotropically distributed in the interior of cells, resulting in important properties at the scale of the whole cell, such as planar cell polarity [21,30]. The assumption of uniform mass distribution hence amounts to neglecting cell polarization. Including the dynamics of cell polarization is of course important in a number of biological situations and will be considered in future work.

Cell shape is described by a shape tensor defined as

$$G_{ij}^\alpha = \frac{1}{n} \sum_{\mu=1}^n \Delta x_i^{\alpha\mu} \Delta x_j^{\alpha\mu}, \quad (1)$$

where $\Delta \mathbf{r}^{\alpha\mu} = \mathbf{r}^{\alpha\mu} - \mathbf{r}_\alpha$, with $\mathbf{r}_\alpha = \frac{1}{n} \sum_{\mu} \mathbf{r}^{\alpha\mu}$, and Latin indices i, j denote components. The shape tensor has been used to describe polymer conformation [31] and the structure of foams [32], as well cellular shape in epithelia [22,24]. It quan-

tifies area, perimeter, and elongations of convex polygonal shapes composed of n vertices connected by rigid edges. The limit $n \rightarrow \infty$ corresponds to an ellipse. We define microscopic mass, momentum, and cell shape density fields as

$$\hat{\rho}(\mathbf{r}, t) = \sum_{\alpha\mu} m \delta(\mathbf{r} - \mathbf{r}^{\alpha\mu}(t)), \quad (2)$$

$$\hat{\mathbf{g}}(\mathbf{r}, t) = \sum_{\alpha\mu} \mathbf{p}^{\alpha\mu} \delta(\mathbf{r} - \mathbf{r}^{\alpha\mu}(t)), \quad (3)$$

$$\hat{G}_{ij}(\mathbf{r}, t) = \sum_{\alpha} G_{ij}^\alpha \delta(\mathbf{r} - \mathbf{r}_\alpha(t)), \quad (4)$$

with $m = m_c/n$, and $\mathbf{p}^{\alpha\mu} = m\dot{\mathbf{r}}^{\alpha\mu}$ is the conjugate momentum. Coarse-grained quantities are then defined as $\rho(\mathbf{r}, t) = [\hat{\rho}(\mathbf{r}, t)]_c$, $\mathbf{g}(\mathbf{r}, t) = [\hat{\mathbf{g}}(\mathbf{r}, t)]_c$, and $G_{ij}(\mathbf{r}, t) = [\hat{G}_{ij}(\mathbf{r}, t)]_c$ and correspond to macroscopic continuum fields describing the system on length scales large compared to both the size of the particles and their mean separation. Note that since the microscopic single-cell shape tensor \mathbf{G}^α has dimensions of length squared, the density of cellular shape tensor G_{ij} is dimensionless. As we will see below, the trace of the shape tensor density provides a measure of the density of cell perimeter, while its traceless part, $\tilde{G}_{ij} = G_{ij} - \frac{1}{2}\delta_{ij}\text{Tr}[\mathbf{G}]$, captures both cell anisotropy and local alignment of elongated cells.

The cellular shape tensor can be written in terms of its eigenvalues as

$$G_{ij}^\alpha = \frac{1}{2}(\lambda_1^\alpha + \lambda_2^\alpha)\delta_{ij} + (\lambda_1^\alpha - \lambda_2^\alpha)(\hat{v}_i^\alpha \hat{v}_j^\alpha - \frac{1}{2}\delta_{ij}), \quad (5)$$

where $\lambda_1^\alpha > \lambda_2^\alpha$ and \hat{v}^α is the eigenvector of the largest eigenvalue. Its traceless part can be written in terms of the local molecular alignment tensor, $\tilde{Q}_{ij}^\alpha = (\lambda_1^\alpha - \lambda_2^\alpha)Q_{ij}^\alpha$, where $Q_{ij}^\alpha = (\hat{v}_i^\alpha \hat{v}_j^\alpha - \frac{1}{2}\delta_{ij})$.

For regular n -sided polygons, the shape tensor is diagonal with $\lambda_1^\alpha = \lambda_2^\alpha$. In this case the cell area $A_\alpha^{(n)}$ and perimeter $P_\alpha^{(n)}$ can be expressed in terms of the invariants of the tensor \mathbf{G}^α as

$$A_\alpha^{(n)} = \frac{n}{2} \sin\left(\frac{2\pi}{n}\right) \sqrt{\det[\mathbf{G}^\alpha]}, \quad (6)$$

$$P_\alpha^{(n)} = \sqrt{2n} \sin\left(\frac{\pi}{n}\right) \sqrt{\text{Tr}[\mathbf{G}^\alpha]}. \quad (7)$$

The derivation of Eqs. (6) and (7) is given in Appendix E. Single-cell anisotropy is measured by $M_\alpha = \lambda_1^\alpha - \lambda_2^\alpha$ which vanishes for regular polygons. To quantify single-cell elongation independently of alignment of elongated cells, we follow Ref. [24], albeit with a slightly different definition of the shape tensor, and introduce an anisotropy density field defined as

$$\hat{M}(\mathbf{r}, t) = \sum_{\alpha} M_\alpha \delta(\mathbf{r} - \mathbf{r}_\alpha(t)) \quad (8)$$

and the associated coarse grained field $M(\mathbf{r}, t) = [\hat{M}(\mathbf{r}, t)]_c$. Work on Vertex and Voronoi models of confluent biological tissue, as well as multiphase fields models, has demonstrated the correlation between tissue fluidity and anisotropy of single-cell shape, as quantified here by M . In Vertex models, this anisotropy provides an order parameter for the solid-liquid transition [14,15].

In the following, we construct hydrodynamic equations for a fluid of deformable particles that couple structural changes encoded in cell shape and alignment of elongated cells to flow. The dynamics of the fluid on scales large compared to the cell

size and mean cell separation is described in terms of a few continuum fields: the mass density ρ , the momentum density \mathbf{g} , the single-cell anisotropy density M , and the cell-shape tensor density G_{ij} .

III. POISSON-BRACKET FORMULATION OF CONTINUUM DYNAMICS

Here we briefly summarize the Poisson-bracket (PB) formalism. Consider a system whose microscopic dynamics is determined by canonically conjugate positions \mathbf{r}^α and momenta \mathbf{p}^α . We describe the dynamics in terms of a few microscopic density fields $\hat{\Psi}^a(\mathbf{r}, t; \{\mathbf{r}^\alpha\}, \{\mathbf{p}^\alpha\})$, for $a = 1, 2, \dots$. These fields are chosen to be either hydrodynamic fields associated with conserved quantities, broken symmetry fields, or quasihydrodynamic fields that decay on timescales large compared to microscopic ones. In the specific case of interest here $\{\hat{\Psi}^a\} = (\hat{\rho}, \hat{\mathbf{g}}, \hat{G}_{ij}, \hat{M})$. The dynamics of the corresponding coarse-grained fields $\Psi^a(\mathbf{r}, t) = [\hat{\Psi}^a(\mathbf{r}, t; \{\mathbf{r}^\alpha\}, \{\mathbf{p}^\alpha\})]_c$ is governed by the equations

$$\partial_t \Psi^a(\mathbf{r}, t) = V^a(\mathbf{r}, t) + D^a(\mathbf{r}, t), \quad (9)$$

where V^a and D^a represent the nondissipative and dissipative parts of the dynamics, respectively. The reactive term V^a is given by

$$V^a(\mathbf{r}) = - \int_{\mathbf{r}'} \{\Psi^a(\mathbf{r}), \Psi^b(\mathbf{r}')\} \frac{\delta \mathcal{F}}{\delta \Psi^b(\mathbf{r}')}, \quad (10)$$

where $\mathcal{F}[\{\Psi^a\}]$ is the free energy,

$$\{\Psi^a(\mathbf{r}), \Psi^b(\mathbf{r}')\} = [\{\hat{\Psi}^a(\mathbf{r}), \hat{\Psi}^b(\mathbf{r}')\}]_c, \quad (11)$$

and

$$\{\hat{\Psi}^a(\mathbf{r}), \hat{\Psi}^b(\mathbf{r}')\} = \sum_{\alpha i} \left[\frac{\partial \hat{\Psi}^a(\mathbf{r})}{\partial p_i^\alpha} \frac{\partial \hat{\Psi}^b(\mathbf{r}')}{\partial r_i^\alpha} - \frac{\partial \hat{\Psi}^a(\mathbf{r})}{\partial r_i^\alpha} \frac{\partial \hat{\Psi}^b(\mathbf{r}')}{\partial p_i^\alpha} \right]. \quad (12)$$

Finally, the dissipative term in the kinetic equation is controlled by all the neglected microscopic degrees of freedom and can be written as

$$D^a(\mathbf{r}) = -\Gamma^{ab} \frac{\delta \mathcal{F}}{\delta \Psi^b(\mathbf{r})}. \quad (13)$$

The dissipation tensor Γ^{ab} is in general a functional of the $\{\Psi^a\}$ and their gradients. It is a phenomenological quantity controlled by the requirement that $\partial_t \Psi^a$ can couple only to driving forces $\frac{\delta \mathcal{F}}{\delta \Psi^b(\mathbf{r})}$ that have different sign under time reversal, to guarantee that such terms describe dissipation. Close to equilibrium it is a symmetric tensor, and it must obey Onsager's principle [33].

A. Poisson brackets

The calculation of the PB of mass and momentum density is straightforward and can be found in the literature [26], with

the result

$$\begin{aligned} \{\rho(\mathbf{r}), g_i(\mathbf{r}')\} &= \rho(\mathbf{r}') \partial_i \delta(\mathbf{r} - \mathbf{r}'), \\ \{g_i(\mathbf{r}), g_j(\mathbf{r}')\} &= -\partial'_i [\delta(\mathbf{r} - \mathbf{r}') g_j(\mathbf{r}')] + \partial_j \delta(\mathbf{r} - \mathbf{r}') g_i(\mathbf{r}'). \end{aligned} \quad (14)$$

The main PBs to be calculated here are those involving the fields describing cellular shape. The details of the derivation are shown in Appendix C, with the result

$$\begin{aligned} \{G_{ij}(\mathbf{r}), g_k(\mathbf{r}')\} &= \partial_k [G_{ij}(\mathbf{r}') \delta(\mathbf{r} - \mathbf{r}')] \\ &\quad - [G_{il}(\mathbf{r}) \delta_{jk} + G_{jl}(\mathbf{r}) \delta_{ik}] \partial_l \delta(\mathbf{r} - \mathbf{r}'), \end{aligned} \quad (15)$$

$$\begin{aligned} \{M(\mathbf{r}), g_i(\mathbf{r}')\} &= [\partial_i M(\mathbf{r})] \delta(\mathbf{r} - \mathbf{r}') - \frac{2R(\mathbf{r})}{M(\mathbf{r})} \\ &\quad \times \tilde{G}_{ij}(\mathbf{r}) \partial_j \delta(\mathbf{r} - \mathbf{r}'), \end{aligned} \quad (16)$$

where we have defined $R(\mathbf{r}, t) = [\text{Tr}[\hat{\mathbf{G}}(\mathbf{r}, t)]]_c$.

To calculate $\{M(\mathbf{r}), g_i(\mathbf{r}')\}$ we have used the identity $\tilde{G}_{ik} \tilde{G}_{kj}^\alpha = \frac{M_\alpha^2}{4} \delta_{ij}$, where the tilde denotes the traceless part of a rank-2 tensor, $\tilde{G}_{ij} = G_{ij} - \frac{1}{2} \delta_{ij} \text{Tr}[\mathbf{G}]$. This allows us to write

$$M_\alpha \{M_\alpha \delta(\mathbf{r} - \mathbf{r}^\alpha), g_i(\mathbf{r}')\} = 2\tilde{G}_{kl}^\alpha \{\tilde{G}_{kl}^\alpha \delta(\mathbf{r} - \mathbf{r}^\alpha), g_i(\mathbf{r}')\}. \quad (17)$$

Finally, the other PBs can be obtained using the identity

$$\{\Psi_n(\mathbf{r}), \Psi_m(\mathbf{r}')\} = -\{\Psi_m(\mathbf{r}'), \Psi_n(\mathbf{r})\}. \quad (18)$$

B. Reactive terms

To evaluate the various contributions to the continuum dynamics, we need to specify the free energy of the system. In general, this has the form

$$\begin{aligned} \mathcal{F} &= \mathcal{F}_K + \mathcal{F}_V \\ &= \int_{\mathbf{r}} \left[\frac{\mathbf{g}^2}{2\rho} + f(\rho, M, \nabla M, G_{ij}, \nabla G_{ij}) \right], \end{aligned} \quad (19)$$

where the first term is the kinetic part and the free energy density f depends on the fields and their gradients.

Using the expressions for the PBs we can then evaluate the reactive terms V^a , with the result

$$V^\rho = -\nabla \cdot (\rho \mathbf{v}), \quad (20)$$

$$\begin{aligned} V_i^g &= -\partial_j (\rho v_i v_j) - \rho \partial_i \frac{\delta \mathcal{F}_V}{\delta \rho} + (\partial_i M) \frac{\delta \mathcal{F}_V}{\delta M} + (\partial_i G_{kl}) \frac{\delta \mathcal{F}_V}{\delta G_{kl}} \\ &\quad + \partial_j \left(2G_{jk} \frac{\delta \mathcal{F}_V}{\delta G_{ik}} - \delta_{ij} G_{kl} \frac{\delta \mathcal{F}_V}{\delta G_{kl}} \right) + 2\partial_j \left(\frac{R}{M} \tilde{G}_{ij} \frac{\delta \mathcal{F}_V}{\delta M} \right), \end{aligned} \quad (21)$$

$$V_{ij}^G = -\nabla \cdot (G_{ij} \mathbf{v}) + G_{ik} \partial_k v_j + G_{jk} \partial_k v_i, \quad (22)$$

$$V^M = -\mathbf{v} \cdot \nabla M + \frac{2R}{M} \tilde{G}_{ij} \partial_i v_j. \quad (23)$$

The elastic and density couplings in Eq. (21) can be rewritten in a more familiar form as gradients of pressure and of an elastic stress. The details can be found in Appendix B, where

it is shown that we can write

$$-\rho \partial_i \frac{\delta \mathcal{F}_V}{\delta \rho} + (\partial_i M) \frac{\delta \mathcal{F}_V}{\delta M} + (\partial_i G_{kl}) \frac{\delta \mathcal{F}_V}{\delta G_{kl}} = -\partial_i p + \partial_j \sigma_{ij}^E, \quad (24)$$

where the pressure p and the elastic stress σ_{ij}^E , that plays the role of the Ericksen stress of nematic liquid crystals, are given by

$$p = \rho \frac{\delta \mathcal{F}_V}{\delta \rho} - f, \quad (25)$$

$$\sigma_{ij}^E = -\frac{\partial f}{\partial \nabla_j M} \nabla_i M - \frac{\partial f}{\partial \nabla_j G_{kl}} \nabla_i G_{kl}. \quad (26)$$

The last two terms in Eq.(21) correspond to gradients of a reactive elastic stress σ_{ij}^G , given by

$$\sigma_{ij}^G = 2 \frac{R}{M} \tilde{G}_{ij} \frac{\delta \mathcal{F}_V}{\delta M} + 2 G_{jk} \frac{\delta \mathcal{F}_V}{\delta G_{ik}} - \delta_{ij} G_{kl} \frac{\delta \mathcal{F}_V}{\delta G_{kl}}. \quad (27)$$

The reactive term for the momentum density equation can then be written as

$$V_i^g = -\partial_j (\rho v_i v_j) - \partial_i p + \partial_j (\sigma_{ij}^G + \sigma_{ij}^E). \quad (28)$$

C. Dissipative terms

There is no dissipative term for the mass density ρ if it is conserved. Dissipative terms in the momentum equation must be odd under time reversal and hence must couple to gradients of velocity. In general, shape anisotropy and alignment of elongated cells will entail anisotropic viscosity coefficients, as in liquid crystals. For simplicity, here we only introduce two viscosities to account for shear (η) and bulk (η_b) deformations, and write

$$D_i^g = \partial_j \sigma_{ij}^D, \quad (29)$$

with

$$\sigma_{ij}^D = 2\eta D_{ij} + \eta_b \delta_{ij} \nabla \cdot \mathbf{v}, \quad (30)$$

where D_{ij} is the symmetrized and traceless rate of strain tensor,

$$D_{ij} = \frac{1}{2} (\partial_i v_j + \partial_j v_i - \delta_{ij} \nabla \cdot \mathbf{v}). \quad (31)$$

Dissipative couplings in the equations for the shape density tensor G_{ij} and the shape anisotropy field M must be even under time reversal and hence can couple to M , G_{ij} , and their gradients. Dissipation will arise from topological rearrangements, as well as from birth/death events when density conservation is broken. In general we can write

$$D_{ij}^G = -\Gamma_{ijkl}^{GG} \frac{\delta \mathcal{F}_V}{\delta G_{kl}} - \Gamma_{ij}^{GM} \frac{\delta \mathcal{F}_V}{\delta M}, \quad (32)$$

$$D^M = -\Gamma^{MM} \frac{\delta \mathcal{F}_V}{\delta M} - \Gamma_{ij}^{MG} \frac{\delta \mathcal{F}_V}{\delta G_{ij}}. \quad (33)$$

The kinetic coefficients Γ^{ab} can generally depend on the shape tensor and anisotropy density field. To linear order in these

fields, a general form is given by

$$\Gamma_{ijkl}^{GG} = \frac{M}{2\gamma_G} (\delta_{ik} \delta_{jl} + \delta_{jk} \delta_{il}) + \frac{1}{\gamma_1} (\delta_{ik} G_{jl} + \delta_{jk} G_{il} + \delta_{il} G_{jk} + \delta_{jl} G_{ik}), \quad (34)$$

$$\Gamma_{ij}^{GM} = \Gamma_{ij}^{MG} = \frac{G_{ij}}{\gamma_2}, \quad (35)$$

$$\Gamma^{MM} = \frac{1}{\gamma_M} + \frac{M}{\gamma_3}, \quad (36)$$

where the kinetic coefficients γ_i , for $i = G, M, 1, 2, 3$, encode the characteristic timescales of dissipative processes. For simplicity we have assumed $\Gamma_{ij}^{GM} = \Gamma_{ij}^{MG}$ although in general the parameters controlling the relaxation in these terms could differ. Note that the second term in Eq. (34) has the form introduced in Ref. [34] for the kinetic coefficient describing the relaxation of the conformation tensor in a polymer suspension.

IV. FINAL EQUATIONS

Putting it all together, we now write the final form of the equations we have obtained. It is convenient to write

$$\partial_i v_j = D_{ij} + \omega_{ij} + \frac{1}{2} \delta_{ij} \nabla \cdot \mathbf{v}, \quad (37)$$

where D_{ij} is the rate of strain tensor given in Eq. (31) and ω_{ij} is the vorticity,

$$\omega_{ij} = \frac{1}{2} (\partial_i v_j - \partial_j v_i). \quad (38)$$

The set of continuum equations for our fluid of deformable cells is then given by

$$\partial_t \rho = -\nabla \cdot \rho \mathbf{v}, \quad (39)$$

$$\rho (\partial_t + \mathbf{v} \cdot \nabla) v_i = -\partial_i p + \partial_j (\sigma_{ij}^G + \sigma_{ij}^E + \sigma_{ij}^D), \quad (40)$$

$$\frac{d}{dt} M = \frac{2R}{M} \tilde{G}_{ij} D_{ij} - \Gamma^{MM} \frac{\delta \mathcal{F}_V}{\delta M} - \Gamma_{ij}^{MG} \frac{\delta \mathcal{F}_V}{\delta G_{ij}}, \quad (41)$$

$$\frac{D}{Dt} G_{ij} = G_{ik} D_{kj} + D_{ik} G_{kj} - \Gamma_{ijkl}^{GG} \frac{\delta \mathcal{F}_V}{\delta G_{kl}} - \Gamma_{ij}^{GM} \frac{\delta \mathcal{F}_V}{\delta M}. \quad (42)$$

We have defined

$$\begin{aligned} \frac{d}{dt} &= \partial_t + \mathbf{v} \cdot \nabla, \\ \frac{D}{Dt} &= \frac{d}{dt} - [\boldsymbol{\omega}, \cdot], \end{aligned} \quad (43)$$

where $\frac{d}{dt}$ is the convective derivative and $[\boldsymbol{\omega}, \cdot]$ is the corotational derivative.¹

The equation for the shape tensor G_{ij} contains couplings to flow vorticity and strain rate which control the tendency of extended and deformable particles to rotate with flow and align with streamlines. The shape tensor G_{ij} plays a role similar to that of the conformation tensor in a polymer suspension [31]. In fact, if we ignore the additional anisotropy density field M ,

¹For tensors ω_{ij} and D_{ij} , the commutator is defined as $[\boldsymbol{\omega}, \mathbf{D}]_{ij} = \omega_{ik} D_{kj} - D_{ik} \omega_{kj}$

the equations derived here for a fluid of deformable particles have the same structure as a one-fluid model of viscoelastic polymer solutions [34]. Unlike in models of polymer suspensions, however, the coefficient of the coupling to strain rate, known in that context as the slip parameter [31], is found to be simply equal to 1 in our PB formulation.

It is also convenient to separate the dynamics of G_{ij} in that of its trace and deviatoric part. The corresponding equations are given by

$$\begin{aligned} \frac{d}{dt}R &= 2\tilde{G}_{ij}D_{ji} - \Gamma_{ikl}^{GG} \frac{\delta\mathcal{F}_V}{\delta G_{kl}} - \Gamma_{ii}^{GM} \frac{\delta\mathcal{F}_V}{\delta M}, \quad (44) \\ \frac{D}{Dt}\tilde{G}_{ij} &= RD_{ij} + \tilde{G}_{ik}D_{kj} + D_{ik}\tilde{G}_{kj} - \delta_{ij}\tilde{G}_{kl}D_{kl} \\ &\quad - \left[\Gamma^{GG} : \frac{\delta\mathcal{F}_V}{\delta\mathbf{G}} \right]_{ij}^{\text{ST}} - \left[\Gamma^{GM} \right]_{ij}^{\text{ST}} \frac{\delta\mathcal{F}_V}{\delta M}, \quad (45) \end{aligned}$$

where $[\cdot]^{\text{ST}}$ denotes the symmetrized and traceless part of the tensor. These equations need to be completed by an expression for the free energy \mathcal{F}_V in terms of the shape tensor and anisotropy density field. Such an expression of course depends on the system of interest. In the next section we consider the specific case of a model of dense biological tissues.

V. CELLULAR TISSUE

Confluent biological tissue, where cells are tightly packed, with no intervening gaps, has been modeled extensively using Vertex or Voronoi models that describe cells as irregular polygons tessellating the plane [8–10]. The behavior of the tissue is controlled by an energy that describes the tendency of each cell to adjust its area A_α and perimeter P_α to target values A_0 and P_0 , given by

$$E_V = \sum_{\alpha} \left[\frac{\kappa_A}{2} (A_\alpha - A_0)^2 + \frac{\kappa_P}{2} (P_\alpha - P_0)^2 \right], \quad (46)$$

with κ_A and κ_P stiffness parameters. The first term arises from tissue incompressibility in three dimensions, and the second captures the interplay of cell-cell adhesion and cortical contractility. By scaling lengths with $\sqrt{A_0}$ and energies with $\kappa_A A_0^2$, the scaled energy of each cell is given by

$$\epsilon_\alpha = \frac{1}{2}(a_\alpha - 1)^2 + \frac{r}{2}(p_\alpha - p_0)^2, \quad (47)$$

with $p_0 = P_0/\sqrt{A_0}$ the target shape parameter and $r = \kappa_P/(\kappa_A A_0)$.

Numerical studies of this energy have identified a rigidity transition at a critical value p_0^* of the target shape parameter between a rigid, solid-like state for $p_0 < p_0^*$ to a fluid state for $p_0 > p_0^*$. Single-cell anisotropy as quantified by the mean cell-shape index $q = \langle P_\alpha/\sqrt{A_\alpha} \rangle$, with the brackets denoting an average over all cells, provides an order parameter for the transition. Czajkowski *et al.* [24] derived a mean-field model of this rigidity transition, albeit using a different definition of the cell shape tensor G_{ij}^c as compared to the one used here. The derivation carried out with our definition is outlined in Appendix D. The result is a quartic Landau-type free energy density f_M where the the cell shape anisotropy density M

plays the role of an order parameter, given by

$$f_M = \frac{\alpha(p_0)}{2}M^2 + \frac{\beta}{4}M^4, \quad (48)$$

where $\alpha(p_0)$ vanishes at $p_0 = p_0^*$ and $\beta > 0$. The definition of the shape tensor of individual cells affects only the precise values of these parameters that also depend on the reference polygonal shape, but does not change the form of the free energy density nor the value of p_0^* . The free energy given in Eq. (48) is obtained by assuming small deformations from regular polygons and constant cell perimeter. It predicts a mean-field transition at $\alpha = 0$ from a state where cells are isotropic ($M = 0$) $\alpha > 0$ or $p_0 < p_0^*$ (the solid state) to a state where cells are anisotropic ($M = \sqrt{-\alpha/\beta}$) for $\alpha < 0$ or $p_0 > p_0^*$ (the liquid state).

This work suggests a phenomenological free energy for a confluent tissue that captures both fluctuations in the cell anisotropy density M that quantifies the liquid-solid transition and the shape tensor density \tilde{G}_{ij} that quantifies alignment of elongated cell as

$$\begin{aligned} \mathcal{F}_c &= \int_{\mathbf{r}} \left[\frac{\alpha(p_0)}{2}M^2 + \frac{\beta}{4}M^4 + \frac{K}{2}(\nabla M)^2 \right. \\ &\quad \left. + \frac{\chi}{2}\text{Tr}[\tilde{\mathbf{G}}^2] + \frac{K_G}{2}(\partial_j\tilde{G}_{ik})^2 \right]. \quad (49) \end{aligned}$$

We do not include terms of order $\text{Tr}[\tilde{\mathbf{G}}^2]^2$ as we do not expect any nematic order of cellular shapes in the absence of externally applied or actively generated internal stresses. Also, we have assumed constant cell perimeter, corresponding to $R = \text{Tr}[\mathbf{G}] = \text{const}$. In general, the various parameters in \mathcal{F}_c will depend on R .

It is important to stress that \tilde{G}_{ij} and M are not independent. The traceless tensor \tilde{G}_{ij} can be written as

$$\tilde{G}_{ij} = S_G(n_i n_j - \frac{1}{2}\delta_{ij}), \quad (50)$$

which defines the director field $\mathbf{n}(\mathbf{r}, t)$ associated with alignment of elongated cells and the magnitude S_G of orientational order. Cell alignment can occur only if cells are elongated ($M \neq 0$), hence $S_G(M)$ must vanish when $M = 0$. We assume $S_G = MS$, where S plays the role of a nematic order parameter for orientational order of elongated cells. Clearly, S is defined only in states where M is finite.

Cell sheets commonly interact with a frictional substrate that eliminates momentum conservation. Frictional drag with the substrate generally exceeds inertial forces, and the Navier-Stokes equation for the momentum is replaced by a Stokes equation quantifying force balance on each fluid element. Within this overdamped limit, and considering a minimal form for the various dissipative kinetic coefficients, the tissue dynamics is governed by²

$$\partial_t \rho = -\nabla \cdot (\rho \mathbf{v}), \quad (51)$$

$$\xi v_i = -\partial_i p + \partial_j (\sigma_{ij}^G + \sigma_{ij}^E + \sigma_{ij}^D), \quad (52)$$

$$\frac{d}{dt}M = 2\frac{R}{M}\tilde{G}_{ij}D_{ij} - \frac{1}{\gamma_M}\frac{\delta\mathcal{F}_c}{\delta M} - \frac{\tilde{G}_{ij}}{\gamma_2}\frac{\delta\mathcal{F}_c}{\delta\tilde{G}_{ij}}, \quad (53)$$

²We consider here uniaxial systems.

$$\begin{aligned} \frac{D}{Dt} \tilde{G}_{ij} &= RD_{ij} + \tilde{G}_{ik} D_{kj} + D_{ik} \tilde{G}_{kj} - \delta_{ij} \tilde{G}_{kl} D_{kl} \\ &\quad - \frac{M}{\gamma_G} \frac{\delta \mathcal{F}_c}{\delta \tilde{G}_{ij}} - \frac{\tilde{G}_{ij}}{\gamma_2} \frac{\delta \mathcal{F}_c}{\delta M}, \end{aligned} \quad (54)$$

where ξ is the frictional drag and

$$\frac{\delta \mathcal{F}_c}{\delta M} = (\alpha + \beta M^2)M - K \nabla^2 M, \quad (55)$$

$$\frac{\delta \mathcal{F}_c}{\delta \tilde{G}_{ij}} = \chi \tilde{G}_{ij} - K_G \nabla^2 \tilde{G}_{ij}. \quad (56)$$

It is useful to consider a simplified form of the equations obtained by retaining only lowest order terms in fields and gradients. In this case the Stokes equation and the equations for the shape fields can be written in the explicit form

$$\Gamma \mathbf{v} = -\nabla p + \eta \nabla^2 \mathbf{v} + \eta_b \nabla \nabla \cdot \mathbf{v} + \nabla \cdot \boldsymbol{\sigma}^G, \quad (57)$$

$$\frac{d}{dt} M = 2 \frac{R}{M} \tilde{G}_{ij} D_{ij} - \frac{1}{\gamma_M} (\alpha + \beta M^2) M + D \nabla^2 M, \quad (58)$$

$$\begin{aligned} \frac{D}{Dt} \tilde{G}_{ij} &= RD_{ij} + \tilde{G}_{ik} D_{kj} + D_{ik} \tilde{G}_{kj} - \delta_{ij} \tilde{G}_{kl} D_{kl} \\ &\quad - r M \tilde{G}_{ij} + D_G \nabla^2 \tilde{G}_{ij}, \end{aligned} \quad (59)$$

where $D = \Gamma_M K$, $D_G = \Gamma K_G$, $r = \chi / \gamma_G + \alpha / \gamma_2$, and

$$\boldsymbol{\sigma}_{ij}^G = 2R(\alpha + \beta M^2) \tilde{G}_{ij} + \frac{1}{2} \delta_{ij} \chi S_G^2. \quad (60)$$

The single-cell anisotropy field M here plays the role of tissue fluidity. The first term on the RHS of Eq. (58) captures the fact that shear deformations, coupled to local cell alignment, can increase cell anisotropy, driving fluidification. The second term describes relaxation to the ground state controlled by the tissue free energy, with a cost for spatial variations in local fluidity controlled by the stiffness D . The reactive terms in Eq. (59) describe flow alignment of elongated cell shape. The term proportional to r describes changes of cell shape tensor due to dissipative processes, such as topological rearrangements, at a rate proportional to the tissue fluidity M . The last term in Eq. (59) describes the stiffness against deformations of local cell alignment. The prefactor to \tilde{G}_{ij} in Eq. (60) represents the zero-frequency tissue shear modulus and vanishes at the transition, corresponding to fluidization of the tissue.

Finally, in a confluent tissue the cell number density $n = \rho / m_c$ is slaved to the mean cell area $\langle A_\alpha \rangle$ with $n = 1 / \langle A_\alpha \rangle$. For cells that are only slightly deformed from regular polygons, $\langle A_\alpha \rangle \simeq \sqrt{\det[\mathbf{G}]} \approx \text{Tr}[\mathbf{G}]$, where we have used Eq. (A4). The density equation, Eq (51), can therefore equivalently be written as an equation for the cell area or for $|G| \equiv \det[\mathbf{G}]$, given by

$$(\partial_t + \mathbf{v} \cdot \nabla) |G| = |G| \nabla \cdot \mathbf{v}. \quad (61)$$

VI. CONCLUSION

Using the Poisson-bracket formalism, we have derived hydrodynamic equations for a fluid of deformable particles in two dimensions. Shape fluctuations are described by two continuum fields: (1) a coarse-grained scalar field that captures single-particle anisotropy, and (2) a shape tensor field that

quantifies both particle elongation and nematic alignment of elongated particles.

We have specifically applied the model to sheets of dense biological tissue, where single-cell anisotropy was recently identified as the order parameter for a solid-liquid transition driven by the interplay of cortex contractility and cell-cell adhesion [14,15]. In other words, in confluent tissue single-cell anisotropy is effectively an experimentally accessible measure of the rheological properties of the tissue, with isotropic cell shapes identifying the solid or jammed state and anisotropic shapes corresponding to a liquid. Previous work has examined the dynamics of a coarse-grained cell shape tensor and its coupling to mechanical stresses [22]. This work did not, however, distinguish between a tissue of elongated, but isotropically oriented cells and one where the cells are elongated and also aligned in a state with nematic liquid crystalline order. The distinguishing ingredient of our work is to distinguish the dynamics of tissue fluidity, as quantified by the single-cell anisotropy field, from that of cell alignment, and examine the interplay between flow, which can be either externally applied or induced by internal active processes, fluidity, and nematic order of cell shapes. Our equations hence provide a starting point for quantifying the rheology of biological tissue. Future extensions needed to develop a complete framework of tissue rheology include the coupling to the dynamics of polarized cell motility and the inclusion of structural rearrangements arising from cell division and death.

Finally, the equations developed here provide a hydrodynamic model for fluids of deformable particles, capable of accounting for both the dynamics of small shape deformations and density changes.

ACKNOWLEDGMENTS

M.C.M. thanks Max Bi, James Cochran, Suzanne Fielding, and Holger Stark for illuminating discussions. This work was supported by the National Science Foundation through award DMR-2041459.

APPENDIX A: USEFUL IDENTITIES

The eigenvalues of a 2×2 symmetric matrix G_{ij} are given by

$$\lambda_{1,2} = \frac{1}{2}(G_{xx} + G_{yy}) \pm \frac{1}{2} \sqrt{(G_{xx} - G_{yy})^2 + 4G_{xy}^2} \quad (A1)$$

and

$$\lambda_1 - \lambda_2 = \sqrt{(G_{xx} - G_{yy})^2 + 4G_{xy}^2}, \quad (A2)$$

$$\lambda_1 \lambda_2 = G_{xx} G_{yy} - G_{xy}^2. \quad (A3)$$

We can then show that the following identities apply

$$(\lambda_1 - \lambda_2)^2 = [\text{Tr} \mathbf{G}]^2 - 4 \det \mathbf{G}, \quad (A4)$$

$$(\lambda_1 - \lambda_2)^2 = 2\text{Tr}[\mathbf{G}^2] - [\text{Tr} \mathbf{G}]^2 = 2\text{Tr}[\tilde{\mathbf{G}}^2]. \quad (A5)$$

Finally, for a regular polygon, G_{ij} is always diagonal and $\lambda_1 = \lambda_2 = \lambda$. In this case Eq. (A4) gives $\text{Tr} \mathbf{G} = 2\sqrt{\det \mathbf{G}}$. For small deformations from a regular polygon $\text{Tr} \mathbf{G} \sim 2\sqrt{\det \mathbf{G}}$,

which implies that we can think of $\text{Tr}\mathbf{G}$ as either a measure of square of cell perimeter or a measure of cell area.

APPENDIX B: ELASTIC STRESS AND PRESSURE

It is convenient to rewrite some of the term in the reactive part \mathbf{V}^s of the momentum density equation given in Eq. (21) to express them as gradients of pressure and an elastic stress. The goal is to rewrite the following terms:

$$\delta V_i^s \equiv -\rho \partial_i \frac{\delta \mathcal{F}_V}{\delta \rho} + (\partial_i M) \frac{\delta \mathcal{F}_V}{\delta M} + (\partial_i G_{kl}) \frac{\delta \mathcal{F}_V}{\delta G_{kl}}. \quad (\text{B1})$$

By relating functional derivatives of \mathcal{F}_V to derivatives of the free energy density f , which is a function of the hydrodynamic fields and their gradients, we can write

$$-\rho \nabla_i \frac{\delta \mathcal{F}_V}{\delta \rho} = -\nabla_i \left(\rho \frac{\partial f}{\partial \rho} \right) + \frac{\partial f}{\partial \rho} \nabla_i \rho, \quad (\text{B2})$$

$$\begin{aligned} (\nabla_i M) \frac{\delta \mathcal{F}_V}{\delta M} &= (\nabla_i M) \left(\frac{\partial f}{\partial M} - \nabla_j \frac{\partial f}{\partial \nabla_j M} \right) \\ &= \frac{\partial f}{\partial M} \nabla_i M - \nabla_j \left[(\nabla_i M) \frac{\partial f}{\partial \nabla_j M} \right] \\ &\quad + \frac{\partial f}{\partial \nabla_j M} \nabla_i (\nabla_j M), \end{aligned} \quad (\text{B3})$$

$$\begin{aligned} (\nabla_i G_{kl}) \frac{\delta \mathcal{F}_V}{\delta G_{kl}} &= (\nabla_i G_{kl}) \left(\frac{\partial f}{\partial G_{kl}} - \nabla_j \frac{\partial f}{\partial \nabla_j G_{kl}} \right) \\ &= \frac{\partial f}{\partial G_{kl}} \nabla_i G_{kl} - \nabla_j \left[(\nabla_i G_{kl}) \frac{\partial f}{\partial \nabla_j G_{kl}} \right] \\ &\quad + \frac{\partial f}{\partial \nabla_j G_{kl}} \nabla_i (\nabla_j G_{kl}). \end{aligned} \quad (\text{B4})$$

Combining these three terms, and using

$$\begin{aligned} \nabla_i f &= \frac{\partial f}{\partial \rho} \nabla_i \rho + \frac{\partial f}{\partial M} \nabla_i M + \frac{\partial f}{\partial \nabla_j M} \nabla_i (\nabla_j M) \\ &\quad + \frac{\partial f}{\partial G_{kl}} \nabla_i G_{kl} + \frac{\partial f}{\partial \nabla_j G_{kl}} \nabla_i (\nabla_j G_{kl}), \end{aligned} \quad (\text{B5})$$

we can write

$$\delta V_i^s = -\nabla_i p + \nabla_j \sigma_{ij}^E \quad (\text{B6})$$

in terms of the pressure p and an elastic stress σ_{ij}^E , given by

$$p = \rho \frac{\partial f}{\partial \rho} - f, \quad (\text{B7})$$

$$\sigma_{ij}^E = -\frac{\partial f}{\partial \nabla_j M} \nabla_i M - \frac{\partial f}{\partial \nabla_j G_{kl}} \nabla_i G_{kl}. \quad (\text{B8})$$

The stress σ_{ij}^E plays the role of the Ericksen stress of nematic liquid crystals.

APPENDIX C: EVALUATION OF POISSON BRACKETS

First, we show the details of the calculation of the fundamental PB $\{G_{ij}^\alpha \delta(\mathbf{r} - \mathbf{r}^\alpha), g_k(\mathbf{r}')\}$. To evaluate the PB we use the following:

$$\frac{\partial \Delta x_i^{\alpha\nu}}{\partial x_j^{\beta\mu}} = \delta^{\alpha\beta} \delta_{ij} \left(\delta^{\mu\nu} - \frac{1}{n} \right), \quad (\text{C1})$$

$$\frac{\partial}{\partial x_j^{\beta\mu}} \delta(\mathbf{r} - \mathbf{r}^\alpha) = -\frac{\delta^{\alpha\beta}}{n} \partial_j \delta(\mathbf{r} - \mathbf{r}^\alpha), \quad (\text{C2})$$

$$\begin{aligned} \delta(\mathbf{r} - \mathbf{r}^\alpha) &= \delta(\mathbf{r} - \mathbf{r}^{\alpha\mu} - \Delta \mathbf{r}^{\alpha\mu}) \\ &= \delta(\mathbf{r} - \mathbf{r}^\alpha) - \Delta x_i^{\alpha\mu} \partial_i \delta(\mathbf{r} - \mathbf{r}^{\alpha\mu}) + O(\Delta x^2 \nabla^2). \end{aligned} \quad (\text{C3})$$

We write

$$\{G_{ij}^\alpha \delta(\mathbf{r} - \mathbf{r}^\alpha), g_k(\mathbf{r}')\} = -\sum_{\beta, \nu} \frac{\partial G_{ij}^\alpha \delta(\mathbf{r} - \mathbf{r}^\alpha)}{\partial x_k^{\beta\nu}} \delta(\mathbf{r}' - \mathbf{r}^{\beta\nu}). \quad (\text{C4})$$

Then

$$\begin{aligned} \frac{\partial G_{ij}^\alpha \delta(\mathbf{r} - \mathbf{r}^\alpha)}{\partial x_k^{\beta\nu}} &= -\frac{1}{n} \delta^{\alpha\beta} G_{ij}^\alpha \partial_k \delta(\mathbf{r} - \mathbf{r}^\alpha) \\ &\quad + \frac{1}{n} \delta^{\alpha\beta} \delta(\mathbf{r} - \mathbf{r}^\alpha) (\delta_{ik} \Delta x_j^{\alpha\nu} + \delta_{jk} \Delta x_i^{\alpha\nu}). \end{aligned} \quad (\text{C5})$$

Inserting Eq. (C5) into Eq. (C4) and using that $\sum_\mu \Delta \mathbf{r}^{\alpha\mu} = 0$, we obtain

$$\{G_{ij}^\alpha \delta(\mathbf{r} - \mathbf{r}^\alpha), g_k(\mathbf{r}')\} = G_{ij}^\alpha [\partial_k \delta(\mathbf{r} - \mathbf{r}^\alpha)] \frac{1}{n} \sum_\nu \delta(\mathbf{r}' - \mathbf{r}^{\alpha\nu}) - \delta(\mathbf{r} - \mathbf{r}^\alpha) \frac{1}{n} \sum_\nu (\delta_{ik} \Delta x_j^{\alpha\nu} + \delta_{jk} \Delta x_i^{\alpha\nu}) \delta(\mathbf{r}' - \mathbf{r}^{\alpha\nu}). \quad (\text{C6})$$

Finally, using

$$\begin{aligned} \delta(\mathbf{r} - \mathbf{r}^{\alpha\nu}) &= \delta(\mathbf{r} - \mathbf{r}^\alpha - \Delta \mathbf{r}^{\alpha\nu}) \\ &\approx \delta(\mathbf{r} - \mathbf{r}^\alpha) - \Delta x_k^{\alpha\nu} \partial_k \delta(\mathbf{r} - \mathbf{r}^\alpha), \end{aligned} \quad (\text{C7})$$

we obtain

$$\begin{aligned} \{G_{ij}^\alpha \delta(\mathbf{r} - \mathbf{r}^\alpha), g_k(\mathbf{r}')\} &= G_{ij}^\alpha \delta(\mathbf{r}' - \mathbf{r}^\alpha) \partial_k \delta(\mathbf{r} - \mathbf{r}^\alpha) + \delta(\mathbf{r} - \mathbf{r}^\alpha) \\ &\quad \times (\delta_{ik} G_{jl}^\alpha + \delta_{jk} G_{il}^\alpha) \partial_l' \delta(\mathbf{r}' - \mathbf{r}^\alpha). \end{aligned} \quad (\text{C8})$$

From this one can immediately obtain Eq. (15).

To evaluate the PB $\{M(\mathbf{r}), g_k(\mathbf{r}')\}$ we let $G_{ij}^\alpha = \frac{I_\alpha}{2} \delta_{ij} + \tilde{G}_{ij}^\alpha$, with $I_\alpha = \hat{G}_{kk}^\alpha$ and $\tilde{G}_{ij}^\alpha = M_\alpha (v_i^\alpha v_j^\alpha - \frac{1}{2} \delta_{ij})$ and use the following identities:

$$\tilde{G}_{ik}^\alpha \tilde{G}_{kj}^\alpha = \frac{M_\alpha^2}{4} \delta_{ij}, \quad (\text{C9})$$

$$\tilde{G}_{ik}^\alpha \tilde{G}_{ki}^\alpha = \frac{M_\alpha^2}{2}. \quad (\text{C10})$$

We can then write

$$M_\alpha \{M_\alpha \delta(\mathbf{r} - \mathbf{r}^\alpha), g_k(\mathbf{r}')\} = 2\tilde{G}_{ij}^\alpha \{ \tilde{G}_{ij}^\alpha \delta(\mathbf{r} - \mathbf{r}^\alpha), g_k(\mathbf{r}') \}. \quad (\text{C11})$$

Using Eq. (C8), we find³

$$\begin{aligned} & \{ \tilde{G}_{ij}^\alpha \delta(\mathbf{r} - \mathbf{r}^\alpha), g_k(\mathbf{r}') \} \\ &= \tilde{G}_{ij}^\alpha \delta(\mathbf{r}' - \mathbf{r}^\alpha) \partial_k \delta(\mathbf{r} - \mathbf{r}^\alpha) + \delta(\mathbf{r} - \mathbf{r}^\alpha) \\ & \quad \times (\delta_{ik} \tilde{G}_{jl}^\alpha + \delta_{jk} \tilde{G}_{il}^\alpha - \delta_{ij} \tilde{G}_{kl}^\alpha) \partial_l' \delta(\mathbf{r}' - \mathbf{r}^\alpha) \\ & \quad + \frac{I_\alpha}{2} (\delta_{ik} \delta_{jl} + \delta_{jk} \delta_{il} - \delta_{ij} \delta_{kl}) \delta(\mathbf{r} - \mathbf{r}^\alpha) \partial_l' \delta(\mathbf{r}' - \mathbf{r}^\alpha). \end{aligned} \quad (\text{C12})$$

and

$$\begin{aligned} & \{ M_\alpha \delta(\mathbf{r} - \mathbf{r}^\alpha), g_k(\mathbf{r}') \} \\ &= M_\alpha \delta(\mathbf{r}' - \mathbf{r}^\alpha) \partial_k \delta(\mathbf{r} - \mathbf{r}^\alpha) + M_\alpha \delta(\mathbf{r} - \mathbf{r}^\alpha) \partial_k' \delta(\mathbf{r}' - \mathbf{r}^\alpha) \\ & \quad + \frac{2I_\alpha \tilde{G}_{kl}^\alpha}{M_\alpha} \delta(\mathbf{r} - \mathbf{r}^\alpha) \partial_l' \delta(\mathbf{r}' - \mathbf{r}^\alpha). \end{aligned} \quad (\text{C13})$$

The PB $\{M(\mathbf{r}), g_k(\mathbf{r}')\}$ is then given by

$$\begin{aligned} \{M(\mathbf{r}), g_k(\mathbf{r}')\} &= \delta(\mathbf{r} - \mathbf{r}') \partial_k M(\mathbf{r}) \\ & \quad - 2 \left[\sum_\alpha \frac{I_\alpha \tilde{G}_{kl}^\alpha}{M_\alpha} \delta(\mathbf{r} - \mathbf{r}^\alpha) \right] \partial_l \delta(\mathbf{r} - \mathbf{r}') \end{aligned} \quad (\text{C14})$$

and involves a new field

$$\sum_\alpha \frac{I_\alpha \tilde{G}_{kl}^\alpha}{M_\alpha} \delta(\mathbf{r} - \mathbf{r}^\alpha) = \sum_\alpha I_\alpha \left(v_i^\alpha v_j^\alpha - \frac{1}{2} \delta_{ij} \right) \delta(\mathbf{r} - \mathbf{r}^\alpha). \quad (\text{C15})$$

We will need to make approximations to close the equations. We will approximate as follows:

$$\sum_\alpha \frac{I_\alpha \tilde{G}_{kl}^\alpha}{M_\alpha} \delta(\mathbf{r} - \mathbf{r}^\alpha) \approx \frac{R(\mathbf{r}) \tilde{G}_{ij}(\mathbf{r})}{M(\mathbf{r})}. \quad (\text{C16})$$

APPENDIX D: MEAN-FIELD THEORY OF VERTEX MODEL

Following Ref. [24], we construct a mean-field free energy by rewriting the *single-cell* Vertex model energy in terms of the cell anisotropy parameter M_α . Let us define

$$M_\alpha = \lambda_1^\alpha - \lambda_2^\alpha, \quad (\text{D1})$$

$$R_\alpha = \lambda_1^\alpha + \lambda_2^\alpha, \quad (\text{D2})$$

which gives $\lambda_{1,2}^\alpha = (R_\alpha \pm M_\alpha)/2$. Equations (6) and (7) are exact for regular polygons, but also hold approximately true for slightly deformed polygons where the shape tensor re-

mains diagonal and $M_\alpha/R_\alpha \ll 1$. We can then write

$$P_\alpha \approx \sqrt{2n} \sin\left(\frac{\pi}{n}\right) (\sqrt{\lambda_1^\alpha + \lambda_2^\alpha}) \equiv v(n) \sqrt{R_\alpha}, \quad (\text{D3})$$

$$A_\alpha = \frac{n}{2} \sin\left(\frac{2\pi}{n}\right) \sqrt{\lambda_1^\alpha \lambda_2^\alpha} \equiv \frac{\mu(n)}{2} \sqrt{R_\alpha^2 - M_\alpha^2}. \quad (\text{D4})$$

The single-cell energy can then be written in terms of R_α and M_α as

$$E_\alpha = \frac{K_A}{2} \left(\frac{\mu}{2} \sqrt{R_\alpha^2 - M_\alpha^2} - A_0 \right)^2 + \frac{K_P}{2} (P_\alpha - P_0)^2. \quad (\text{D5})$$

Following Ref. [24], we restrict ourselves to small deformations from a regular polygon and expand $M_\alpha/R_\alpha \ll 1$, with the result

$$\begin{aligned} E_\alpha &= \frac{K_A}{2} \left\{ \left(\frac{\mu R_\alpha}{2} - A_0 \right)^2 + \frac{1}{2} R_\alpha \mu \left(A_0 - \frac{R_\alpha \mu}{2} \right) \left(\frac{M_\alpha}{R_\alpha} \right)^2 \right. \\ & \quad \left. + \frac{R_\alpha \mu}{8} A_0 \left(\frac{M_\alpha}{R_\alpha} \right)^4 + O\left[\left(\frac{M_\alpha}{R_\alpha} \right)^6 \right] \right\} \\ & \quad + \frac{K_P}{2} (v \sqrt{R_\alpha} - P_0)^2. \end{aligned} \quad (\text{D6})$$

We further assume that the cell perimeter is constant, or $P_\alpha = P_0$, hence $R_\alpha = P_0^2/v^2$. Substituting into Eq. (D6), we can rewrite the single-cell energy density $e_\alpha = E_\alpha/A_0$ as

$$e_\alpha = e_0 + \frac{1}{2} \alpha(n, p_0) \left(\frac{M_\alpha}{A_0} \right)^2 + \frac{1}{4} \beta(n, p_0) \left(\frac{M_\alpha}{A_0} \right)^4, \quad (\text{D7})$$

where e_0 is a constant and

$$\alpha(n, p_0) = \frac{\kappa_A A_0^2 \mu^2}{4p_0^2} (p_0^{*2} - p_0^2), \quad (\text{D8})$$

$$\beta(n, p_0) = \frac{\kappa_A A_0^4 \mu v^6}{4p_0^6}, \quad (\text{D9})$$

with $p_0 = P_0/\sqrt{A_0}$ the shape index, our tuning parameter. Also, $\alpha(n, p_0)$ has been written in terms of the critical shape index,

$$p_0^* = v \sqrt{\frac{2}{\mu}} = \sqrt{4n \tan(\pi/n)}. \quad (\text{D10})$$

The limits of these approximations were tested numerically in Ref. [24], where it was shown that Eq. (D7) provides a good description of the model near the transition, where cells are only minimally deformed.

More familiar particulate systems can be tuned between solid and liquid states by changing the density or packing fraction. Confluent tissues have a packing fraction of 1 but can be tuned between liquid and solid states by changing the parameter p_0 that measures the target cell perimeter in units of the target cell area. For $p_0 < p_0^*$ the system is frustrated as cells cannot reach both their target area and perimeter, resulting in finite energy barriers for cellular rearrangements, and the tissue is a solid [13,14]. For $p_0 > p_0^*$ such energy barriers vanish and cells easily exchange neighbors, resulting in a liquid-like state.

The value of critical target shape parameter p_0^* depends on the specific undeformed polygonal shape, with $p_0^* = 4$ for

³Note that the PB of \tilde{G}_{ij} given below is the same as the PB of the quantity R_{ij} of Ref. [26], albeit in two dimensions.

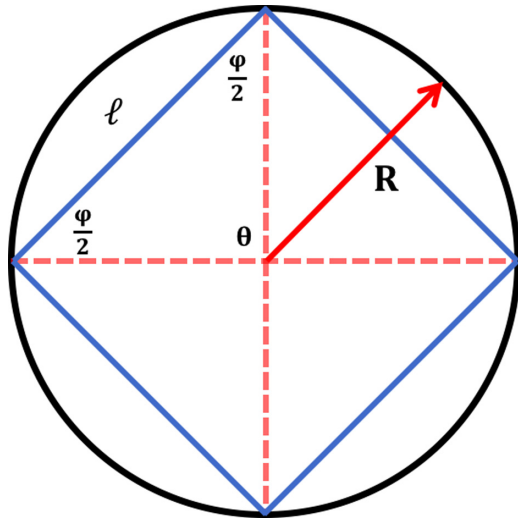


FIG. 2. Regular polygon of side ℓ circumscribed inside a circle of radius R .

squares and $p_0^* = 2\sqrt{2\sqrt{3}} \approx 3.722$ for hexagons. Equation (D8) shows explicitly that α changes sign at $p_0 = p_0^*$, while $\beta > 0$. For $\alpha > 0$ the stable ground state has $M = 0$ and corresponds to a solid-like state of isotropic cells. For $\alpha < 0$ the stable ground state is a fluid of anisotropic cells, with $M/A_0 = \pm\sqrt{-\alpha/\beta}$. At $\alpha = 0$ the system undergoes spontaneous symmetry breaking and fluidizes, choosing one of two equivalent axial direction along which to elongate. Here we have defined M as positive by assuming $\lambda_1 > \lambda_2$, hence breaking from the outset the Ising symmetry of the model.

The nature of this solid-liquid transition has been discussed in the context of Voronoi and Vertex model simulation, where a continuous transition results in fluidization at constant density, as quantified through measurements of energy barriers and mean-square displacement. [14,15].

Finally, it was shown in Ref. [24] that the quartic form given in Eq. (D7) is also obtained by assuming constant cell area, albeit with different expressions for the coefficients α

and β . In both cases the coefficient α changes sign at $p_0 = p_0^*$ and the behavior near the transition is unaffected by the approximation used.

APPENDIX E: DERIVATION OF EQS. (6) AND (7)

The shape tensor approximates a polygonal cell, labeled by α , as an ellipse defined by

$$(\mathbf{r}^\alpha - \mathbf{r}_C^\alpha) \cdot (\mathbf{G}^\alpha)^{-1} (\mathbf{r}^\alpha - \mathbf{r}_C^\alpha)^T = 1, \quad (\text{E1})$$

where \mathbf{r}_C^α is the center of the cell. In a coordinate basis where the tensor is diagonal the equation for the cell boundary is given by

$$\frac{(x - x_0)^2}{\lambda_1} + \frac{(y - y_0)^2}{\lambda_2} = 1, \quad (\text{E2})$$

where $1/\lambda_{1,2}^2$ are the eigenvalues of $\mathbf{G}^{\alpha^{-1}}$ and determine the major and minor semiaxes of the ellipse. For a regular polygon we have $\lambda_1 = \lambda_2 = R^2$, and Eq. (E2) reduces to the equations for a circle of radius R .

Consider a regular n -sided polygon with edges ℓ circumscribed in a circle of radius R , as illustrated in Fig. 2. The polygon has a total interior angle of $(n-2)\pi$. The angle between any two neighboring edges is $\varphi = \frac{(n-2)\pi}{n}$ and the central angle is given by $\theta = \frac{2\pi}{n}$. Elementary trigonometry then yields the following relationships:

$$P = n\ell = 2nR \sin\left(\frac{\pi}{n}\right), \quad (\text{E3})$$

$$A = \frac{n}{2} \sin\left(\frac{2\pi}{n}\right) R^2. \quad (\text{E4})$$

For regular polygons the eigenvalues of the shape tensor are equal, with $\lambda_1 = \lambda_2 = R^2$, and Eqs. (E4) and (E3) can be recast in the forms given in Eqs. (6) and (7) for the area and perimeter of regular polygons. Although Eq. (7) does not hold for general deformed ellipses, it is the first-order approximation of the exact expression given by a hypergeometric function and has been validated numerically for small deformations [22,35].

-
- [1] T. Lecuit and P. F. Lenne, *Nat. Rev. Mol. Cell Biol.* **8**, 633 (2007).
 [2] D. J. Durian, *Phys. Rev. Lett.* **75**, 4780 (1995).
 [3] S. Cohen-Addad, R. Höhler, and O. Pitois, *Annu. Rev. Fluid Mech.* **45**, 241 (2013).
 [4] J. Mattsson, H. M. Wyss, A. Fernandez-Nieves, K. Miyazaki, Z. Hu, D. R. Reichman, and D. A. Weitz, *Nature (London)* **462**, 83 (2009).
 [5] D. Vlassopoulos and M. Cloitre, *Curr. Opin. Colloid Interface Sci.* **19**, 561 (2014).
 [6] F. Graner and J. A. Glazier, *Phys. Rev. Lett.* **69**, 2013 (1992).
 [7] A. J. Kabla, *J. R. Soc., Interface* **9**, 3268 (2012).
 [8] H. Honda, M. Tanemura, and T. Nagai, *J. Theor. Biol.* **226**, 439 (2004).
 [9] L. Hufnagel, A. A. Teleman, H. Rouault, S. M. Cohen, and B. I. Shraiman, *Proc. Natl. Acad. Sci. USA* **104**, 3835 (2007).
 [10] R. Farhadifar, J.-C. Röper, B. Aigouy, S. Eaton, and F. Jülicher, *Curr. Biol.* **17**, 2095 (2007).
 [11] E. Hannezo, J. Prost, and J.-F. Joanny, *Proc. Natl. Acad. Sci. USA* **111**, 27 (2014).
 [12] N. Murisic, V. Hakim, I. G. Kevrekidis, S. Y. Shvartsman, and B. Audoly, *Biophys. J.* **109**, 154 (2015).
 [13] D. Bi, J. H. Lopez, J. M. Schwarz, and M. L. Manning, *Soft Matter* **10**, 1885 (2014).
 [14] D. Bi, J. H. Lopez, J. M. Schwarz, and M. L. Manning, *Nat. Phys.* **11**, 1074 (2015).
 [15] D. Bi, X. Yang, M. C. Marchetti, and M. L. Manning, *Phys. Rev. X* **6**, 021011 (2016).
 [16] E. Teomy, D. A. Kessler, and H. Levine, *Phys. Rev. E* **98**, 042418 (2018).
 [17] S. Kim, M. Pochitaloff, Georgina-Stooke-Vaughan, and O. Campàs, *bioRxiv* (2020).

- [18] A. Boromand, A. Signoriello, J. Lowensohn, C. S. Orellana, E. R. Weeks, F. Ye, M. D. Shattuck, and C. S. O'Hern, *Soft Matter* **15**, 5854 (2019).
- [19] M. Doi and T. Ohta, *J. Chem. Phys.* **95**, 1242 (1991).
- [20] A. Sagner, M. Merkel, B. Aigouy, J. Gaebel, M. Brankatschk, F. Jülicher, and S. Eaton, *Curr. Biol.* **22**, 1296 (2012).
- [21] M. Popović, A. Nandi, M. Merkel, R. Etournay, S. Eaton, F. Jülicher, and G. Salbreux, *New J. Phys.* **19**, 033006 (2017).
- [22] S. Ishihara, P. Marcq, and K. Sugimura, *Phys. Rev. E* **96**, 022418 (2017).
- [23] X. Yang, D. Bi, M. Czajkowski, M. Merkel, M L. Manning, and M. C. Marchetti, *Proc. Natl. Acad. Sci. USA* **114**, 12663 (2017).
- [24] M. Czajkowski, D. Bi, M. L. Manning, and M. C. Marchetti, *Soft Matter* **14**, 5628 (2018).
- [25] D. Forster, *Phys. Rev. Lett.* **32**, 1161 (1974).
- [26] H. Stark and T. C. Lubensky, *Phys. Rev. E* **67**, 061709 (2003).
- [27] H. Stark and T. C. Lubensky, *Phys. Rev. E* **72**, 051714 (2005).
- [28] J. A. Park, J. H. Kim, D. Bi, J. A. Mitchel, N. T. Qazvini, K. Tantisira, Chan Y. Park, M. McGill, S. H. Kim, B. Gweon *et al.*, *Nat. Mater.* **14**, 1040 (2015).
- [29] C. Malinverno, S. Corallino, F. Giavazzi, M. Bergert, Q. Li, M. Leoni, A. Disanza, E. Frittoli, A. Oldani, E. Martini *et al.*, *Nat. Mater.* **16**, 587 (2017).
- [30] L. V. Goodrich and D. Strutt, *Development* **138**, 1877 (2011).
- [31] A. N. Beris and B. J. Edwards, *Thermodynamics of Flowing Systems: With Internal Microstructure* (Oxford Engineering Science Series, Oxford, 1994).
- [32] F. Graner, B. Dollet, C. Raufaste, and P. Marmottant, *Eur. Phys. J. E* **25**, 349 (2008).
- [33] S. Ruurds De Groot, *Thermodynamics of Irreversible Processes* (North-Holland, Amsterdam, 1951).
- [34] S. T. Milner, *Phys. Rev. E* **48**, 3674 (1993).
- [35] T. R. Chandrupatla and T. J. Osler, *Math. Sci.* **35**, 122 (2010).